Dyes and Pigments 95 (2012) 776–783

Contents lists available at SciVerse ScienceDirect

Dyes and Pigments

journal homepage: www.elsevier.com/locate/dyepig

Review

Modification of silica nanoparticles with fluorescein hydrozide for Cu(II) sensing

Xiaotong Chen [a,*], Aijun Tong [b]

[a] Institute of Nuclear and New Energy Technology, Tsinghua University, Beijing 100084, PR China
[b] Department of Chemistry, Tsinghua University, Beijing 100084, PR China

ARTICLE INFO

Article history:
Received 5 January 2012
Received in revised form
18 June 2012
Accepted 20 June 2012
Available online 28 June 2012

Keywords:
Silica nanoparticles
Fluorescein hydrozide
Copper(II)
Sensing
Covalent binding
Cu(II)-amplified fluorescence

ABSTRACT

Fluorescein hydrozide modified silica nanoparticles (FH-SNPs, 280–550 nm) were prepared by covalently immobilizing a fluorescein hydrozide (FH) derivative containing organosilyl ligands onto the surface of silica nanoparticles. FT-IR, elemental analysis, SEM microscopy and steady-state fluorescence anisotropy were used to characterize the functionalized FH-SNPs. Upon the addition of Cu(II), the spirolactam ring of FH moiety on the silica surface was opened and a fluorescent product was formed, exhibiting a selective Cu(II)-amplified fluorescence signal. Under the optimized conditions, the linear range of fluorescence intensity for Cu(II) is 5–80 μM (R^2 = 0.992), and the limit detection for Cu(II) is 1.0 μM according to IUPAC definition ($C_{LOD} = 3.3S_b/m$).

1. Introduction

Nanoparticle supports for hybrid organic dyes include silica, titania, alumina, and gold, which lead to pigments of smaller particles and an increase efficiency of dye adsorption [1–3]. Silica provides a hydrophilic surface due to the presence of silanol groups, which are weakly acidic and reactive for chemical modification [4,5]. Hybrid pigments composed of silica and organic dyes are promising substrates for chemical sensors [6–9], adsorption [10–12] and catalysis [13,14]. There are mainly two approaches to synthesize modified silica nanoparticles (SNPs). For the "bottom-up" approach, building blocks are allowed to self-organize into nanoparticle systems with functional properties [15–18]; nanoparticles prepared by water-in-oil microemulsion (*W*/*O*) are monodispersed, uniform in size, and relatively easy to control the size by varying the water to surfactant molar ratio and dynamic properties of microemulsion [19–21]. On the other hand, the direct modification of a dye to silica involves its modification with aminosilane coupling agent to graft silane chain onto silica surface, and then a functional group reacts with the grafted silane groups [22]. By above methods, the silica offers an optically transparent solid support to be chemically modified by target-selective molecules, resulting in a boost in the development of optical sensor such as pH, anions, metal ions and neutral molecules [23–26].

In particular, the detection of Cu(II) by SNPs has received considerable attention, since the analytical significance of trace Cu(II) found in both environmental and biological processes [27–29]. Tonellato and his co workers grafted Cu(II) ligands and a fluorescent dye (8-anilinenaphthalensulfonic acid) to the surface of commercially available silica particles, and the operative range of sensors can be tuned either by switching the ligand units or by modification of components ratio [23]. However, It is well known that the detection mechanisms of Cu(II) were usually based on fluorescence quenching because of its paramagnetic properties, which would not satisfactory for the detecting effect [28,30–32]. Therefore, chemosensors exhibiting a Cu(II)-amplified fluorescence signal are always considered to be more attractive and efficient [33,34].

In this work, we selected a fluorescein hydrozide (FH) as an organic moiety, which was grafted onto the surface of silica nanoparticles to obtain FH-SNPs to detect Cu(II). In 30% (*v*/*v*) water/CH_3CN (10 mM Tris–HCl, pH = 5.2) buffer media, FH-SNPs displayed a fluorescence enhancement at 560 nm in the presence of Cu(II), and a selective detection of Cu(II) over other metal ions was achieved with the detection limit as 1 μM. Moreover, FH-SNPs could be repeatedly used for Cu(II) sensing after regeneration procedures

* Corresponding author. Tel.: +86 10 89796097; fax: +86 10 69771464.
E-mail address: chenxiaotong@mail.tsinghua.edu.cn (X. Chen).

0143-7208/$ – see front matter © 2012 Elsevier Ltd. All rights reserved.
http://dx.doi.org/10.1016/j.dyepig.2012.06.012

by hydrazine solutions, which facilitated a reproducible dye-grafted fluorescent solid sensor for Cu(II) in water and practical samples.

2. Experimental section

2.1. Reagents

Doubly distilled deionized water was used throughout the experiment. All reagents were purchased from commercial suppliers (Beijing Chemical Reagent Co., China; Acros; Fluka) and used without further purification. The solutions of Cu(II), Fe(III), Co(II), Pb(II), Cd(II), Ag(I), Mn(II), Hg(II), Ca(II), Mg(II), Ba(II), K(I) and Zn(II) were prepared from their nitrate salts. The silica nanoparticles were purchased from Wanjing Co., China. Unless otherwise noted, all reagents and solvents used were analytical grade and without further purification.

2.2. Apparatus and spectroscopic measurements

Absorption spectra were determined on a JASCO V-550 UV–vis spectrophotometer. Fluorescence spectra measurements were performed on a JASCO FP-6500 spectrofluorimeter equipped with a xenon discharge lamp, 1 cm quartz cells. NMR spectra were recorded using a JOEL JNM-ECA300 spectrometer operated at 300 MHz. ESI spectra were obtained on an HP 1100 LC-MS spectrometer. Elemental analysis results were gained from Elementar Vario EL (Germany). Scanning electron microscopy (SEM) experiments were performed at JEM 2010. The particle size distributions were constructed with MIORO-PLUS (50 nm–555 μm) light scattering instrument. Nitrogen adsorption–desorption isotherms were measured with a Micrometric ASAP 2020 adsorption analyzer (Norcross, GA). The specific surface areas of the sample membranes were calculated using the multiple-point Brunauer-Emmett-Teller (BET) method. The degree of modification and the silica support coverage with dyes were estimated by FT-IR spectrophotometer (JASCO FI/IR–6200). All measurements were operated at room temperature (about 298 K).

2.3. Synthesis of fluorescein hydrozide

The synthesis route was shown in Scheme 1. Fluorescein hydrozine ($C_{20}H_{16}N_2O_4$, **2**) was prepared as previously reported [35]. Diethyl fluorescein hydrozine-3,6-diacetate ($C_{28}H_{28}N_2O_8$, **3**)

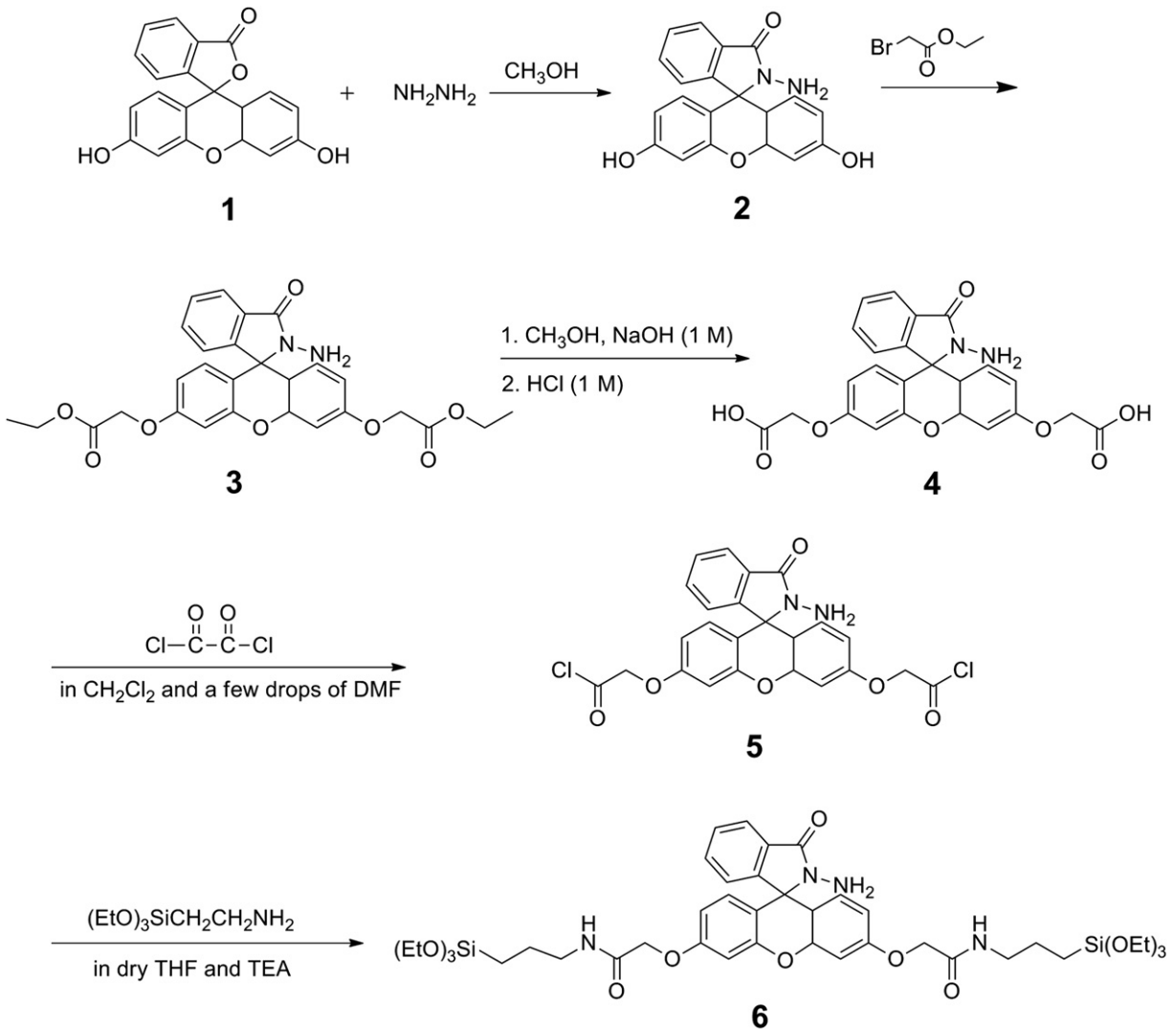

Scheme 1. Chemical structures and synthesis route of **1**–**6**.

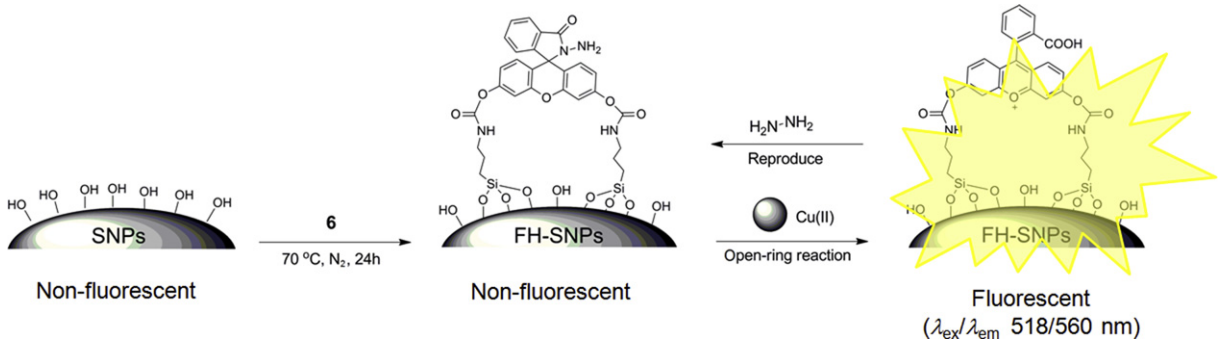

Scheme 2. The fabrication procedure of FH molecules onto the surface of SNPs.

was prepared by adding ethyl bromoacetate (1.6 mL, 14.37 mmol) dropwise into a mixture of 1.30 g (3.76 mmol) of **2** and 1.28 g of K_2CO_3. The mixture was stirred at 70 °C in 15 mL CH_3CN for 2 h. A raw product was obtained by evacuating CH_3CN under reduced pressure, and then washed by 1 M HCl and water each for twice. The purified precipitant was taken by column chromatography on silica gel with ethyldichloroacetate/petroleum ether (2/1) as a developer. The organic layer was then dried over $MgSO_4$, and the removal of the organic solvent in vacuum provided **3** as a light yellow powder with 64% yield (1.83 g). ESI mass spectrometry: *m*/*z* 517.66 ($[M-H]^+$); M^+ calculated 518.42. ^{1}H-NMR ($CDCl_3$), δ (ppm): 1.31 (t, 6H, $J = 7.0$ Hz), 4.28 (q, 4H, $J = 7.1$ Hz), 4.62 (s, 4H), 6.59 (m, 4H), 6.73 (s, 2H), 7.05 (dd, 1H, $J_1 = 5.4$ Hz, $J_2 = 2.9$ Hz), 7.49 (dd, 2H, $J_1 = 5.1$ Hz, $J_2 = 3.1$ Hz). 7.95 (dd, 1H, $J_1 = 5.5$ Hz, $J_2 = 3.1$ Hz). ^{13}C-NMR ($CDCl_3$) δ (ppm): 14.3, 61.7, 65.2, 65.5, 102.3, 111.8, 111.9, 123.4, 123.9, 128.6, 128.9, 129.6, 133.1, 150.8, 153.1, 158.9, 166.4, 168.5.

Fluorescein hydrozine-3,6-diacetic acid ($C_{24}H_{20}N_2O_8$, **4**) was obtained by dissolving **3** in CH_3OH (10 mL) and 1 M NaOH (4.5 mL, 4.5 mmol). The mixture was stirred at room temperature for 1 h and 1 M HCl (4.5 mL, 4.5 mmol) was then added under vigorous stirring. After the removing of CH_3OH solvent under reduced pressure, a white solid precipitation was obtained. **4** was then purified by filtered, washed with water three times and desiccated under vacuum (0.23 g, 86%). ESI mass spectrometry: *m*/*z* 461.29 ($[M-H]^+$); M^+ calculated 462.41. ^{1}H-NMR (DMSO-D_6), δ (ppm): 4.71 (s, 4H), 6.53 (d, 2H, $J = 8.9$ Hz), 6.64 (dd, 2H, $J_1 = 8.9$ Hz, $J_2 = 2.4$ Hz), 6.79 (d, 2H, $J = 2.4$ Hz). 7.05 (dd, 1H, $J_1 = 5.4$ Hz, $J_2 = 2.9$ Hz), 7.49 (dd, 2H, $J_1 = 5.1$ Hz, $J_2 = 3.1$ Hz). 7.79 (dd, 1H, $J_1 = 5.5$ Hz, $J_2 = 3.1$ Hz). ^{13}C-NMR (DMSO-D_6), δ (ppm): 65.0, 65.3, 102.2, 112.1, 112.7, 123.1, 124.0, 128.6, 129.2, 129.8, 133.3, 151.8, 152.3, 158.9, 166.2, 170.5.

Compound **4** was further designed to attach to the triethoxysilane group, which is essential for grafting onto the surface of silica nanoparticles. Fluorescein hydrozine-3,6-diacetyl chloride ($C_{24}H_{18}Cl_2N_2O_6$, **5**) with acetyl chloride was generated from the reaction of **4** *in situ* by reacting with oxalyl chloride (6 equiv). Since **5** is easy to be hydrolyzed in the air, it was immediately added to a solution of dry THF (50 mL) and TEA (0.1 mL) after the removal of organic solvent and excessive oxalyl chloride to obtain fluorescein hydrozine-3,6-bis(*N*-triethoxylsilylpropyl)acetamide($C_{42}H_{62}N_4O_{12}Si_2$, **6**). ESI mass spectrometry: *m*/*z* 869.25 ($[M-H]^+$); M^+ calculated 870.39. ^{1}H-NMR (DMSO-D_6), δ (ppm): 0.53 (t, 4H, $J = 7.1$ Hz), 1.24 (t, 18H, $J = 7.9$ Hz), 1.69 (m, 4H), 3.48 (t, 4H, $J = 7.0$ Hz), 3.85 (q, 12H, $J = 7.9$ Hz), 4.65 (s, 4H), 6.51(d, 2H, $J = 8.9$ Hz), 6.60 (dd, 2H, $J_1 = 8.9$ Hz, $J_2 = 2.4$ Hz), 6.75 (d, 2H, $J = 2.4$ Hz). 7.01 (dd, 1H, $J_1 = 5.4$ Hz, $J_2 = 2.9$ Hz), 7.45 (dd, 2H, $J_1 = 5.1$ Hz, $J_2 = 3.1$ Hz). 7.72 (dd, 1H, $J_1 = 5.5$ Hz, $J_2 = 3.1$ Hz). ^{13}C-NMR (DMSO-D_6), δ (ppm):13.5, 18.2, 25.1, 43.3, 58.0, 65.2, 65.4, 102.5, 111.9, 112.5, 122.5, 124.3, 128.9, 129.5, 129.1, 133.1, 151.3, 152.5, 158.6, 166.6, 170.3.

2.4. Preparation of fluorescein hydrozide modified silica nanoparticles (FH-SNPs)

The synthetic routes for the preparation of sample nanoparticles are schematically shown in Scheme 2. In brief, SNPs were at first dispersed in anhydrous toluene (8 mL); afterwards, **6** (100 mg,

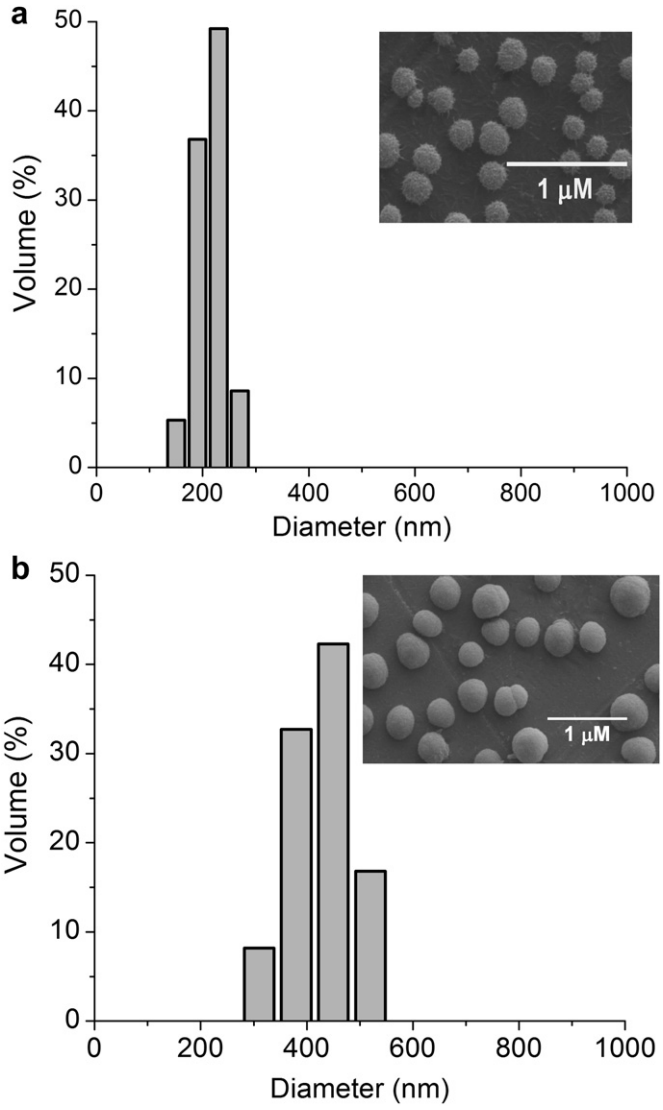

Fig. 1. Particle size distributions and SEM image of (a) unmodified silica and (b) FH-SNPs.

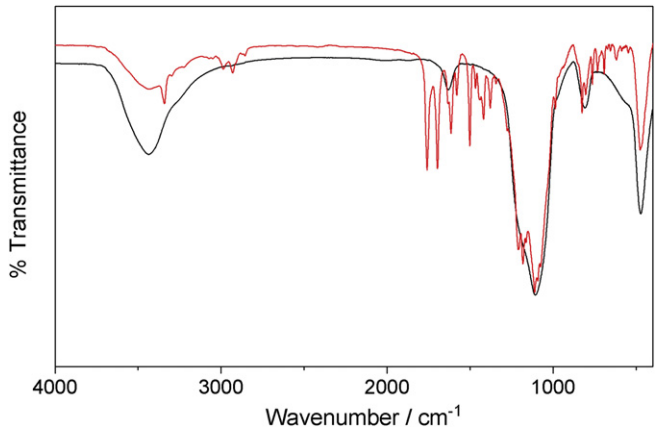

Fig. 2. FT-IR spectra of (black) SNPs and (red) FH-SNPs. (For interpretation of the references to colour in this figure legend, the reader is referred to the web version of this article.)

0.115 mmol) was dissolved in 2 mL anhydrous toluene and added dropwise to SNPs solution. The mixture was stirred under reflux at 70 °C in N_2 environment for 24 h. In the above processes, the triethoxysilyl group of **6** could be covalently attached to the surface of SNPs through hydrolysis reaction [36–38]. The obtained functionalized SNPs were centrifuged for 40 min to remove the supernatant, and then washed with 10 mL of toluene, ethanol, and water in sequence for at least 5 times until the upper solution showed no UV–vis enhancement performance at around 510 nm (which was ascribed to FH molecules). The resulting nanoparticles containing FH moieties (**3**) were designated as FH-SNPs. For control experiments, SNPs containing adsorbed FH was also prepared by dispersed 1 g SNPs in 10 mL FH toluene solution (0.6 mM) under sonication for 30 min, and the toluene was then evaporated under vacuum. The resulting SNPs containing physisorbed FH was named as *ad*FH-SNPs.

3. Results and discussions

3.1. Characterization of FH-SNP

As shown in Fig. 1, the particle size distribution of the unmodified silica shows a single band with the diameter ranging from 130 nm to 240 nm (Fig. 1a); and the surface modification resulted in an increase in the volume contribution ranging from 280 to 550 nm (Fig. 1b). These data were also confirmed by SEM measurements (inset pictures of Fig. 1a and b). For further structural evidence of FH-SNPs, IR spectroscopy was also carried out for both SNPs and FH-SNPs (Fig. 2). For SNPs, IR peaks appeared at around 3436 cm^{-1}, which originated from the O–H stretching vibration of H-bond of surface hydroxyls; and peaks at 1106 cm^{-1}, 806 cm^{-1} and 471 cm^{-1} could be attributed to Si–O–Si vibration absorbance peak, which were almost unchanged after the modification. For FH-SNPs, the peaks at 3436 cm^{-1} became weak, and a new peak at 3350 cm^{-1} appeared, which could be assigned to *sec*-acylamino (–CONH–) group. Moreover, other characteristic peaks of FH molecules could also be observed in FH-SNPs: 2927 cm^{-1}, 2850 cm^{-1} and 1467 cm^{-1} belong to $-CH_2-$ group; 1604 cm^{-1}, 1587 cm^{-1} and 1502 cm^{-1} were ascribed to benzene framework vibration; 1759 cm^{-1} belong to α-substituted ketone peak; and 1699 cm^{-1} was for Ar–CO absorbance peak. These addition peaks from FH molecules provided evidence of the FH attaching to SNPs.

Table 1
The anisotropy values of FH-SNPs and *ad*FH-SNPs in the presence of 10 μM Cu(II).[a]

A	FH-SNPs	*ad*FH-SNPs
518/560	0.382	6.48×10^{-3}

[a] $\lambda_{ex}/\lambda_{em}$ = 518/560 nm c[Cu(II)] = 10 μM; c(FH-SNPs) = c(*ad*FH-SNPs) = 10 mg/mL.

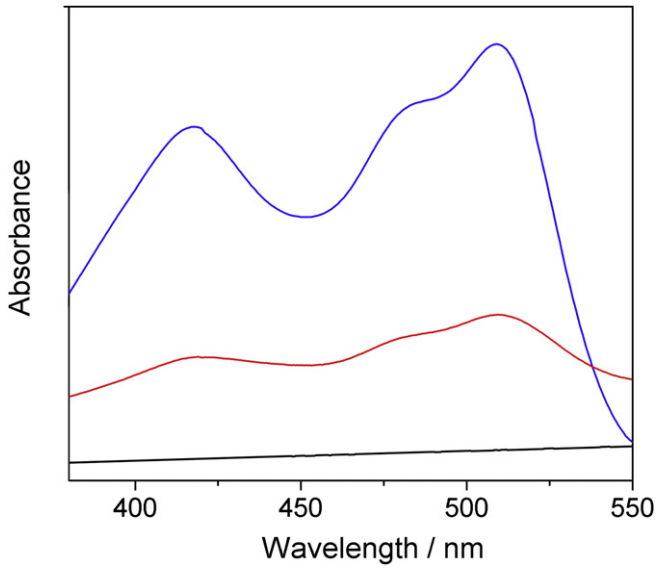

Fig. 3. Absorption spectra of **3** (blue) and FH-SNPs (red) upon the addition of Cu(II) in 30% (v/v) water/CH_3CN (10 mM Tris–HCl buffer, pH = 5.2). The black line is the blank of FH-SNPs. c(**3**) = 10 μM, c(FH-SNPs) = 10 mg/mL, c[Cu(II)] = 12 μM. (For interpretation of the references to colour in this figure legend, the reader is referred to the web version of this article.)

Elemental analysis (Table S1) evidenced the presence of such elements as C, H and N on the silica surface. The presence of nitrogen followed by the structure of compound **6** ($C_{28}H_{32}N_4O_{12}Si_2$). According to the nitrogen content obtained from the elemental analysis results, the loading ratio of FH molecules was found to be 0.6 mmol per gram of FH-SNPs; and the extent of silica surface coverage was calculated as 1.03 μmol/m^2 according to the equation of Berendsen and de Golan [39].

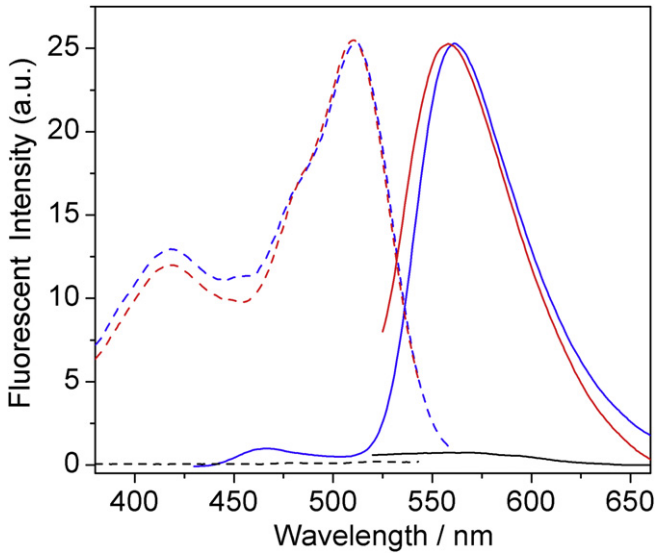

Fig. 4. Normalized excitation (left, dash line) and emission (right, solid line) spectra of **3** (blue line) and FH-SNPs (red line) upon the addition of Cu(II) in 30% (v/v) water/CH_3CN (10 mM Tris–HCl buffer, pH = 5.2). The black line is the FH-SNPs without Cu(II). c(**3**) = 10 μM, c(FH-SNPs) = 10 mg/mL, c[Cu(II)] = 12 μM $\lambda_{ex}/\lambda_{em}$ = 518 nm/560 nm. (For interpretation of the references to colour in this figure legend, the reader is referred to the web version of this article.)

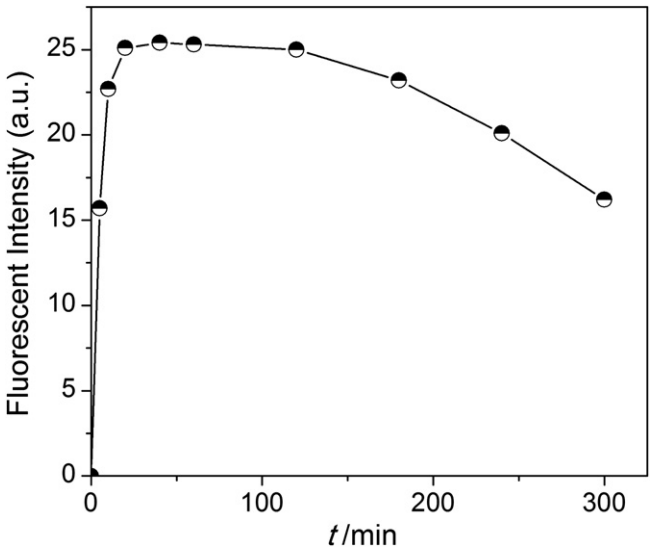

Fig. 5. The time curve of fluorescent signal in 30% (v/v) water/CH_3CN (10 mM Tris–HCl buffer). c(FH-SNPs) = 10 mg/mL, c[Cu(II)] = 10 μM, $\lambda_{ex}/\lambda_{em}$ = 518 nm/560 nm.

3.2. The covalent binding of FH molecules on silica nanoparticles

The formation of covalent bond between FH molecules and SNPs was further confirmed by fluorescence anisotropy measurements, which can provide information on molecular orientation and mobility [40,41]. The degree of anisotropy is determined by measuring fluorescence parallel and perpendicular to the plane of linearly polarized excitation light:

$$r = \frac{I_{II} - I_I}{I_{II} + 2I_I}$$

where I_{II} and I_I are the fluorescence intensities parallel and perpendicular to the direction of the illumination, respectively. The fluorescence anisotropy employed here was based on that the covalent binding FH molecules to silica surface would decrease the rotational mobility, and its anisotropy would approach a higher value. In the presence of 10 μM Cu(II), the anisotropy of FH-SNPs and *ad*FH-SNPs upon Cu(II) addition were measured. Prior to the anisotropy measurement, the sample particles of FH-SNPs and *ad*FH-SNPs were treated as followed: firstly, Cu(II) was introduced by dispersing 0.1 g particles in a 10 μM Cu(II) solution; afterwards, the particles were treated under sonication for 1 h; at last, the anisotropy of sample particles was measured.

As shown in Table 1, there is a great increase of anisotropy value for FH-SNPs compared to *ad*FH-SNPs, indicating a reduced mobility of fluorescein (open-ring structure) after the reaction with Cu(II). Under sonication treatment, the FH molecules adsorbed on silica nanoparticles would be dispersed to solution, whereas for FH-SNPs, the ring-opened fluorescein moiety would be still grafted onto silica surface. Therefore, the formation of covalent linkage between FH molecules and SNPs in FH-SNPs was further confirmed.

3.3. Absorption and fluorescence properties of FH-SNPs

The absorption and fluorescence spectra of **3** and FH-SNPs were measured in 30% (v/v) water/CH_3CN mixture (10 mM Tris–HCl buffer, pH = 5.2). Due to its poor aqueous solubility, **3** could not be well dispersed in mixed solutions with high percentage of water, which dramatically limits its potential applications. To improve the sensory capability in aqueous solution, 70% CH_3CN was used in this study. As shown in Fig. 3, **3** (10 μM) displayed almost no signal in both adsorption (level-off tails demonstrated the scattering effect of FH-SNPs and SNPs) and fluorescence spectra in 30% (v/v) water/CH_3CN mixture (10 mM Tris–HCl buffer, pH = 5.2). Upon the addition of 1.2 equiv of Cu(II), the absorbance was significantly enhanced with the appearance of a new peak at 508 nm, and the fluorescence was also enhanced at 560 nm when excited at 518 nm. Since the absorption and fluorescence spectral shapes of FH-SNPs were close to those of **3** in the presence of Cu(II) (Figs. 3 and 4), the fluorescence of FH-SNPs can be ascribed to **3** moieties on silica surface. Therefore, the fluorescence of FH-SNPs could be used to detect Cu(II) in aqueous solution. The stability of FH-SNPs solution was also investigated as shown in Fig. 5. It could be observed that the fluorescence signal was stable in 2 h. The fluorescence intensity slightly decreased when the time was further extended, which was probably caused by the particle precipitation. Therefore, the optical signals in this study were measured within 2 h to ensure the validity of the experiment data.

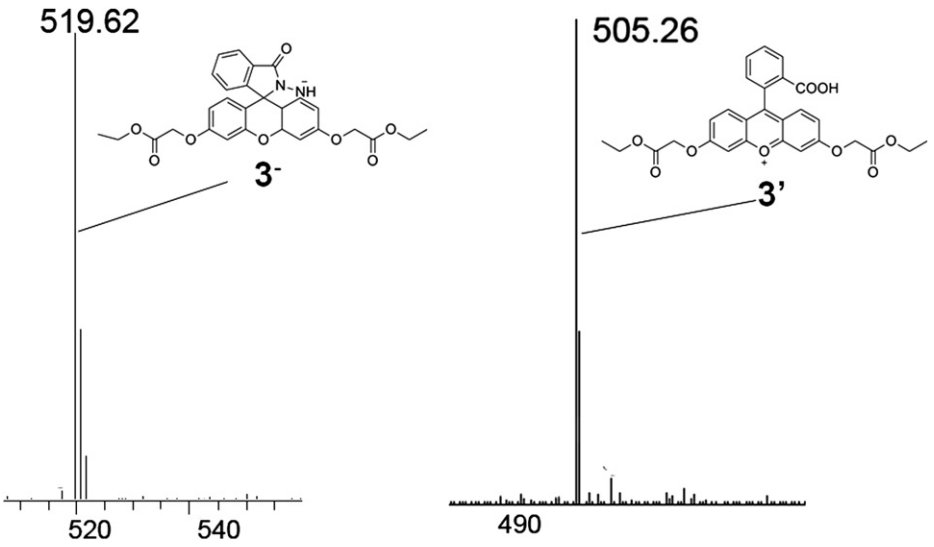

Fig. 6. ESI mass spectra for the spirolactam form **3** (left spectrum, positive) and for the opened ring form **3′** (right spectrum, negative) in the presence of Cu(II) (1.2 equiv).

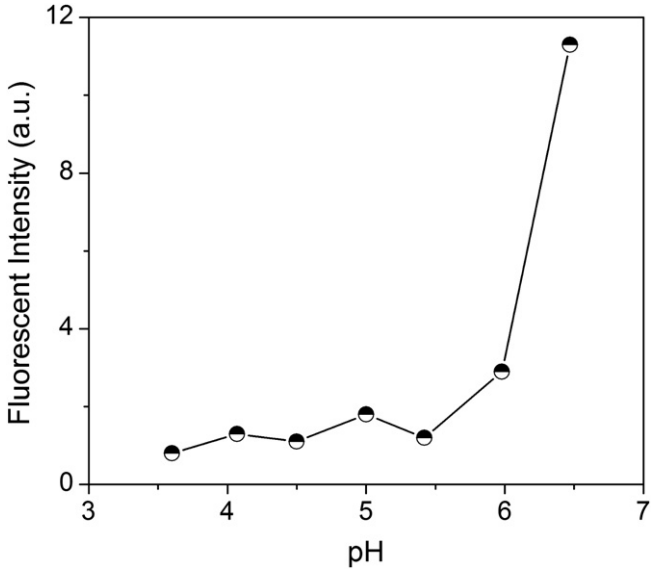

Fig. 7. The pH effect on the fluorescence of FH-SNPs in absence of Cu(II) in 30% (*v*/*v*) water/CH_3CN (10 mM Tris–HCl buffer). *c*(FH-SNPs) = 10 mg/mL, $\lambda_{ex}/\lambda_{em}$ = 518 nm/560 nm.

From the results of ESI mass spectra of **3** and **3**-Cu(II) (Fig. 6), the peak at *m*/*z* = 519.32 (calcd = 519.28) without Cu(II) corresponded to the deprotonation form [**3**–H]$^-$, whereas **3** after Cu(II) addition exhibited peak at *m*/*z* 505.26 (**3′**, calcd = 505.21) could be assigned to the ring-opened form (Scheme 2). Since the peak for the complex form [**3**-Cu(II) calcd = 568.76] hasn't been observed, and the addition of EDTA couldn't restore the fluorescence intensity, the fluorescence-on change of FH-SNPs was probably caused by the formation of ring-opened fluorescein form of **3** moieties after reacting with Cu(II).

When pH was over 5.2, the FH moiety would exhibit open-ring reaction without Cu(II) and increase the background signal (Fig. 7). Therefore, the pH value of the solution was found to be a significant factor for the sensing ability of FH-SNPs. The fluorescence changing

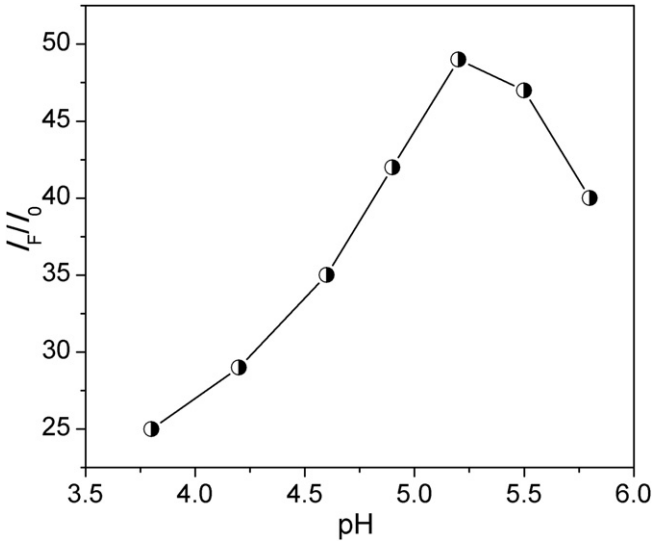

Fig. 8. pH effects on the fluorescence intensity of FH-SNPs with the addition of Cu(II) (10 μM) in 30% (*v*/*v*) water/CH_3CN (10 mM Tris–HCl buffer). pH values are 3.8, 4.2, 4.6, 4.9, 5.2, 5.5 and 5.8; I_0 and I_F are the emission intensities of FH-SNPs without and with Cu(II) addition, respectively. *c*(FH-SNPs) = 10 mg/mL, *c*[Cu(II)] = 10 μM $\lambda_{ex}/\lambda_{em}$ = 518 nm/560 nm.

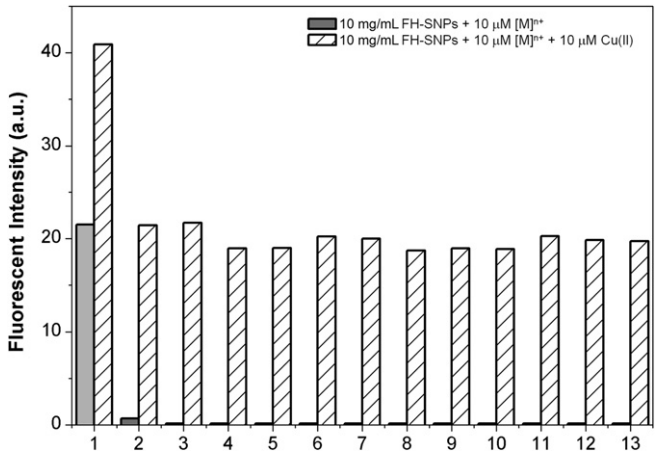

Fig. 9. Fluorescence column spectra of FH-SNPs in 30% (*v*/*v*) water/CH_3CN (10 mM Tris–HCl buffer, pH = 5.2) in the presence of Cu(II) and other metal ions (10 μM). *c*(FH-SNPs) = 10 mg/mL $\lambda_{ex}/\lambda_{em}$ = 518 nm/560 nm. 1: Cu(II), 2: Zn(II), 3: Co(II), 4: Cd(II), 5: Pb(II), 6: Mn(II), 7: Fe(III), 8:Hg(II), 9: Ag(I), 10: Ca(II), 11: Mg(II), 12: Ba(II), 13: K(I).

was examined when the concentration of Cu(II) was 10 μM by varying pH from 3.8 to 5.8 (Fig. 8), and pH 5.2 was selected as the optimized pH value at which maximum I_f/I_0 value could be observed.

3.4. Sensing ability of FH-SNPs for Cu(II)

The sensing ability of FH-SNPs to Cu(II) was studied in CH_3CN/water. Upon the addition of 10 μM Cu(II) to the solution of FH-SNPs, a stable fluorescent signal at 560 nm could be obtained within 10 min and remained constant for 2 h, whereas such fluorescence enhancement could not be observed in the presence of other metal ions such as Zn(II), Co(II), Cd(II), Pb(II), Mn(II), Fe(III), Hg(II), Ag(I), Ca(II), Mg(II), Ba(II), K(I) (Fig. 9). It was also found that higher concentration of Cu(II) was benefit to the rate of the reaction. Under a 15 min stirring time which ensured the accomplishment of the reaction at lower Cu(II) concentration, the calibration curve for the

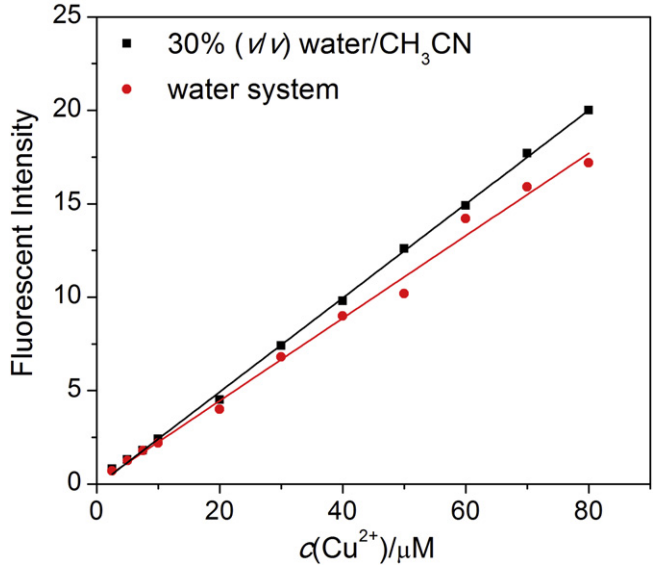

Fig. 10. The linear relationship of fluorescence intensity of FH-SNPs with Cu(II) in 30% (*v*/*v*) water/CH_3CN (10 mM Tris–HCl buffer, pH = 5.2) (black) and water system (red). *c*(FH-SNPs) = 10 mg/mL $\lambda_{ex}/\lambda_{em}$ = 518 nm/560 nm. (For interpretation of the references to colour in this figure legend, the reader is referred to the web version of this article.)

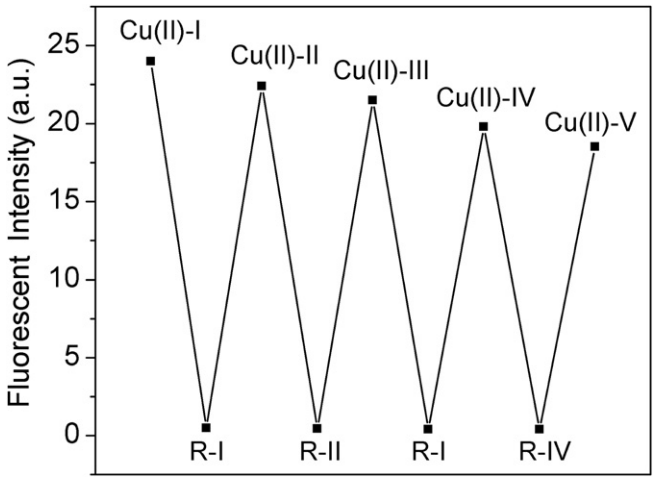

Fig. 11. Regeneration cycles for FH-SNPs upon the addition of 10 μM Cu(II). FH-SNPs is regenerated by being dispersed in 0.1 M hydrazine EtOH solution for 30 min. After the centrifugation, the regenerated FH-SNPs could be used to detect Cu(II) for at least 5 times.

determination of Cu(II) was constructed with fluorescence excitation/emission at 518/560 nm. The linear range was 5–80 μM with a correlation coefficient of $R^2 = 0.992$ (Fig. 10). The detection limit based on the definition by IUPAC ($c_{LOD} = 3S_b/m$), was found to be 1 μM from 10 blank solutions. The relative standard deviation (R.S.D.) for five repeated measurements of 10 μM Cu(II) was 2.6%. The sensing ability was also studied in water systems in consideration of the requirement of practical application, and the detection limit was 1.8 μM, indicating a fair dispersion of silica nanoparticles in water system because of the hydroxyl groups on the surface.

Finally, the reusability of FH-SNPs was examined. The used FH-SNPs could be easily regenerated by being dispersed in 0.1 M hydrazine solution (EtOH) and stirred for 30 min. After the centrifugation and sonication, FH-SNPs could be used to detect Cu(II) with satisfactory effect for at least 5 times (Fig. 11).

3.5. Application of the method

The detection of Cu(II) in tap water and two solution samples were carried out by using FH-SNPs (Table 2). For a general test, 9.50 mL of a sample solution was transferred to a 10 mL tube, and then 0.50 mL 1.0 M buffer stock solution at pH 5.2 and 0.1 g FH-SNPs were added. The system was well mixed under sonication for 0.5 h, and 3.0 mL of this homogeneous system was pippetted into a quartz cell (1 cm × 1 cm) with fluorescence signal measured at $\lambda_{ex}/\lambda_{em}$ 518/560 nm. As summarized in Table 2, the results showed satisfactory results and R.S.D. values (2.3–2.7%) for all the samples.

Table 2
Determination of Cu(II) in environmental samples.[a]

Sample	Cu(II) added (μM)	Cu(II) found (μM)	Recovery (%)	R.S.D (%)
Tap water	8.70	8.90	102	2.5
	37.0	38.5	104	2.6
Sample 1[b] (Cu(II) 8.70 μM)	8.70	17.6	108	2.3
	37.0	47.1	103	2.4
Sample 2[b] (Cu(II) 37.0 μM)	8.70	46.4	102	2.6
	15.0	54.6	105	2.7

[a] Conditions: pH = 5.2. Excitation/emission was performed at 518/560 nm *c*(FH-SNPs) = 10 mg/mL. FH-SNPs is regenerated by being dispersed in 0.1 M hydrazine EtOH solution for 30 min and washed after each use.

[b] Synthetic samples containing other metal ions (μM): K(I) 500, Ca(II) 500, Fe(II) 100, Fe(III) 100, Zn(II) 200, Ni(II) 200, Cd(II) 200, Pb(II) 200. (NO_3^- as anions).

4. Conclusions

In this study, silica nanoparticles functionalized by fluorescein hydrozide (FH-SNPs) were fabricated. Due to the open-ring reaction of FH moiety after reacting with Cu(II) in aqueous solution, FH-SNPs displayed a selective fluorescence enhancement upon the Cu(II) addition, and a linear range of 5–80 μM Cu(II) with a detection limit of 1 μM could be obtained. Also, FH-SNPs could be used as a reusable sensor to monitor Cu(II) in tap water.

Acknowledgement

This work was supported by the National Natural Science Foundation of China (NSFC, no. 20875054), and the young scholar research fund of Tsinghua University (No. 553431001).

Appendix A. Supplementary material

Supplementary data associated with this article can be found, in the online version, at http://dx.doi.org/10.1016/j.dyepig.2012.06.012.

References

[1] Leng B, Zou L, Jiang JB, Tian H. Sensors and Actuators B-Chemical 2009;140:162–9.
[2] Zhang JJ, Riskin M, Freeman R, Tel-Vered R, Balogh D, Tian H, et al. ACS Nano 2011;5:5936–44.
[3] Modrzejewska S, Ciesielczyk F, Jesionowski T. Pigment and Resin Technology 2012;41:71–80.
[4] Jesionowski T, Nowacka M, Ciesielczyk F. Pigment and Resin Technology 2012;41:9–19.
[5] Jesionowski T, Przybylska A, Kurc B, Ciesielczyk F. Dyes and Pigments 2011;89:127–36.
[6] Dziadas M, Nowacka M, Jesionowski T, Jeleń HH. Analytica Chimica Acta 2011;699:66–72.
[7] Andrzejewska A, Krysztafkiewicz A, Jesionowski T. Dyes and Pigments 2007;75:116–24.
[8] Zhang NB, Xu JJ, Xue CG. Journal of Luminescence 2011;9:2021–5.
[9] Guo HQ, Tao SQ. Sensors and Actuators B-Chemical 2007;1:578–82.
[10] An FQ, Gao BJ, Dai X, Wang M, Wang XH. Journal of Hazardous Materials 2011;192:956–62.
[11] Jesionowski T, Binkowski S, Krysztafkiewicz A. Dyes and Pigments 2005;65:267–79.
[12] Anbia M, Salehi S. Dyes and Pigments 2012;94:1–9.
[13] Banerjee S, Santra S. Tetrahedron Letters 2009;50:2037–40.
[14] Sun Y, Yan F, Yang W, Zhao S, Yang W, Sun C. Analytical Bioanalytical Chemistry 2007;387:1565–72.
[15] Mann S. Chemical Communications 2004:1–4.
[16] Hecht S. Angewandte Chemie International Edition 2003;42:24–6.
[17] Stöber W, Fink A, Bohn E. Journal of Colloid Interface Science 1968;26:62–9.
[18] Kurumada K, Kaminura Y, Igarashi K, Umeda N, Kambara H, Yuasa T, et al. Dyes and Pigments 2007;74:433–8.
[19] Bagwe RP, Yang CY, Hilliard LR, Tan WH. Langmuir 2004;20:8336–42.
[20] Zhao XJ, Hilliard LR, Mechery SJ, Wang YP, Bagwe RP, Jin SG, et al. Proceedings of the National Academy of Sciences USA 2004;101:15027–32.
[21] Bagwe RP, Khilar KC. Langmuir 2000;16:905–10.
[22] Van Blaaderen A, Vrij A. Journal of Colloid Interface Science 1993;156:1–18.
[23] Rampazzo E, Brasola E, Marcuz S, Mancin F, Tecilla P, Tonellato U. Journal of Materials Chemistry 2005;15:2687–96.
[24] Mancin F, Rampazzo E, Tecilla P, Tonellato U. Chemistry-A European Journal 2006;12:1844–54.
[25] Ariga K, Vinu A, Hill J, Mori T. Coordination Chemistry Reviews 2007;251:2562–91.
[26] Melde B, Johnson B. Analytical Bioanalytical Chemistry 2010;398:1565–73.
[27] Walkup GK, Imperiali B. Journal of the American Chemical Society 1996;118:3053–4.
[28] Montalti M, Prodi L, Zaccheroni N. Journal of Materials Chemistry 2005;15:2810–4.
[29] Henary MM, Fahrni CJ. Journal of Physical Chemistry A 2002;106:5210–20.
[30] Brasola E, Mancin F, Rampazzo E, Tecilla P, Tonellato U. Chemical Communications 2003:3026–7.
[31] Seo SM, Lee HY, Park MS, Lim JM, Kang DM, Yoon JY, et al. European Journal Inorganic Chemistry 2010;6:843–7.

[32] Zheng JN, Xiao C, Fei Q, Li M, Wang BJ, Feng GD, et al. Nanotechnology 2010; 21:045501–5.
[33] Zong CH, Ai KL, Zhang G, Li HW, Lu LH. Analytical Chemistry 2011;83: 3126–32.
[34] Bonacchi S, Genovese D, Juris R, Montalti M, Prodi L, Rampazzo E, et al. Angewandte Chemie International Edition 2011;50:4056–66.
[35] Chen XT, Li ZF, Xiang Y, Tong AJ. Tetrahedron Letters 2008;49:4697–700.
[36] Lee SJ, Lee JE, Seo J, Jeong IY, Lee SS, Jung JH. Advanced Functional Materials 2007;17:3441–6.
[37] Obare SO, Hollowell RE, Murphy CJ. Langmuir 2002;18:10407–10.
[38] Balaji T, El-Safty SA, Matsunaga H, Hanaoka T, Mizukami F. Angewandte Chemie International Edition 2006;45:7202–8.
[39] Berendsen GE, de Golan L. Journal of Liquid Chromatography and Related Technologies 1978;1:561–86.
[40] Lackowicz JR. Principles of fluorescence spectroscopy. 3rd ed. New York: Springer; 2006. 353–354.
[41] Tleugabulova D, Zhang Z, Chen Y, Brook MA, Brennan JD. Langmuir 2004;20: 848–54.